Journal of Inclusion Phenomena and Molecular Recognition in Chemistry **28:** 95–103, 1997.

Thermal Stability and Decomposition Kinetics of the β-CD Cinnamic Aldehyde Inclusion Complex

JING-HUA LI, NING ZHANG,* XIAO-TAO LI and JIN-YUN WANG
Department of Chemistry, Henan Normal University, Xinxiang, Henan, 453002, P.R. China.

(Received: 8 March 1995; in final form: 13 November 1996)

Abstract. The stability of the β-CD cinnamic aldehyde inclusion complex was investigated by TG and DSC. The weight loss takes place in three stages: dehydration occurs at 50–120 °C; the dissociation of β-CD·C_9H_8O occurs at 200–260 °C; and the decomposition of β-CD begins at 280 °C. The kinetics of the dissociation of cinnamic aldehyde from the β-CD cavity were studied by means of thermogravimetry both at constant temperature and linear increasing temperature. The results show that the dissociation of β-CD·C_9H_8O is dominated by a one-dimensional diffusion process. The activation energy, E, is 160 kJ·mol^{-1}. The pre-exponential factor A is 5.8 × 10^{14} min^{-1}.

Key words: Inclusion complex, β-cyclodextrin, thermal analysis, kinetics.

1. Introduction

Inclusion complexes of β-CD with many guest molecules have been successfully utilized in the food and pharmaceutical industries [1, 2]. So far, many authors laid particular stress on its characteristics in water or its crystal structures in the solid state [3–5]. But the stability and kinetic studies on the inclusion complexes in the solid state present interesting problems in industrial applications. Normally unstable substances, such as aromas, pharmaceuticals and insecticides, are stabilized by the use of inclusion complexes with β-CD. To judge whether β-CD is able to prevent the loss of guest molecules, one criterion is the initial dissociation temperature of guest molecules from β-CD. Sometimes it is more important to determine the final escape temperature of guest molecules from the β-CD cavity. Potential uses are for waste water treatment. Some pollutants in water can be included with β-CD, and then the crystals of the inclusion complex are heated. If the pollutants are able to escape from the β-CD cavity just before the decomposition temperature of β-CD, β-CD can be used again. It is significant to set up a kinetic equation for describing the dissociation process and to explain the driving force of the escape of guest molecules from the β-CD cavity.

Cinnamic aldehyde was chosen as a model guest molecule. This was only because it has suitable size and molecular characteristics. Thermal analysis is a useful method for determining the decomposition temperature and identifying the

* Author for correspondence. Present address: Department of Chemistry, Zhumadian Teachers' College (Zhumadian, 463000, P.R. China).

reaction mechanisms. In this paper, the stability and kinetics of β-CD cinnamic aldehyde were investigated by TGA. The kinetic mechanism of the dissociation of β-CD·C_9H_8O was identified, and the kinetic parameters were obtained.

2. Experimental

2.1. Preparation of the sample

β-CD (purchased from Suzhou government power factory, China) and cinnamic aldehyde (analytical reagent) were dissolved in a 1 : 1 molar ratio in water at 70 °C, then stirred for 1 h at constant temperature. The solution was cooled to room temperature for 24 h and then filtered. The pale yellow crystals were dried for 24 h at 25 °C and seived to less than 190 mesh. The composition was identified by TGA as β-CD·1.08C_9H_8O·6.88H_2O.

2.2. Apparatus and measurements

Thermogravimetric analysis was performed on a WRT-1 microbalance (Shanghai Balancing Instruments Factory). The analytical parameters were: sample mass, about 15 mg; heating rate, 5 °C min^{-1}; chart speed, 4 mm min^{-1}; atmosphere, flowing dried nitrogen 20 ml min^{-1}; sample holder, 5 mm $\times$ 5 mm aluminium crucible.

Differential scanning calorimetry was carried out on a CDR-1 differential scanning calorimeter (Shanghai Balancing Instruments Factory). The experimental conditions were: sample mass, about 5 mg; heating rate, 5 °C min^{-1}; chart speed, 10 mm min^{-1}; atmosphere, static air; reference material, Al_2O_3.

All the thermogravimetric data (α, 0.1 $\sim$0.9) were analyzed on an AT-386 computer. A linear regression program was used.

3. Results and Discussion

3.1. Stability of the inclusion complexes

Figure 1 shows the TG and DSC curves of β-CD·11H_2O and β-CD·C_9H_8O·7H_2O.

The TG curve of β-CD·11H_2O indicates that all of the constitutional water is released at 50–120 °C with a weight loss of 14.85%. At 270 °C, a further weight loss indicates the decomposition of β-CD. The endothermic peaks at 90 and 340 °C in the DSC curve are consistent with the dehydration of β-CD·11H_2O and the decomposition of β-CD on the TG curve, respectively.

Differing from β-CD·11H_2O, β-CD·C_9H_8O·7H_2O has a 8.72% weight loss at 50–120 °C as well as a 10.2% weight loss at 200–260 °C, and a larger weight loss at 280 °C. The three steps correspond to the dehydration, the dissociation of cinnamic aldehyde from β-CD cavity and the decomposition of β-CD, respectively. The DSC curve has four smaller endothermic peaks at 50–120 °C. These indicate that the energies for dehydration of the internal and external water molecules

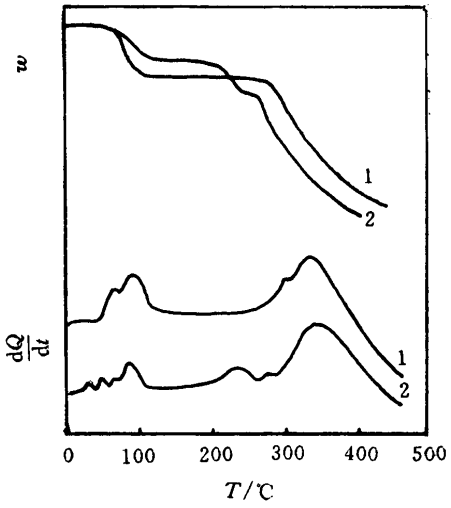

Figure 1. TGA and DSC curves of β-CD·11H_2O(1) and β-CD·C_9H_8O·7H_2O(2).

are different. In addition, the oxygen atoms, whose electronegativity is larger in cinnamic aldehyde molecules, will form stronger hydrogen bonds with adjacent water molecules. So the seven water molecules are distributed in four different positions. The smooth endothermic peak at 200–260 °C corresponds to the loss of cinnamic aldehyde from the β-CD cavity. The low endothermic peak indicates that the attraction between β-CD and cinnamic aldehyde is a weak intermolecular force.

3.2. IDENTIFICATION OF THE KINETIC MECHANISM

According to the thermal analysis results, the decomposition of β-CD·C_9H_8O·7H_2O takes place in three stages.

1: β-CD·C_9H_8O·7H_2O(s) → β-CD·C_9H_8O(s) + 7H_2O(g)
2: β-CD·C_9H_8O(s) → β-CD(s) + C_9H_8O(g)
3: the decomposition of β-CD.

The kinetic mechanism of the second stage, an interesting problem in industrial uses, was analyzed. The isothermal method was conducted as follows: the temperature was raised to 120 °C at a heating rate of 5 °C min^{-1}, and kept at 120 °C for 20 min in order to dehydrate the sample, then the temperature was rapidly raised to 200 °C at a heating rate of 160 °C min^{-1}. The isothermal TG curve at 200 °C was recorded. Using similar methods, the isothermal TG curves were recorded at 210, 220 and 230 °C, respectively.

Table I. Kinetic models of the decomposition of solids.

$g(\alpha)$	Symbol	Rate-determining process
α^2	D_1	one-dimensional diffusion
$\alpha + (1-\alpha)\ln(1-\alpha)$	D_2	two-dimensional diffusion
$[1-(1-\alpha)^{1/3}]^2$	D_3	three-dimensional diffusion (Jander function)
$1-2/3\alpha-(1-\alpha)^{2/3}$	D_4	three-dimensional diffusion (G–B function)
$\ln[\alpha/(1-\alpha)]$	Au	autocatalytic reaction (P–T function)
$1-(1-\alpha)^{1/n}$	Rn	phase boundary reaction, n =1, 2, 3 (one-, two-, three-dimensional respectively)
$[-\ln(1-\alpha)]^{1/m}$	Am	random nucleation and subsequent growth (Avrami–Erofeyev function)

The kinetics of a solid-state decomposition reaction can be represented by the general equation:

$$\mathrm{d}\alpha/\mathrm{d}t = kf(\alpha) \tag{1}$$

or

$$g(\alpha) = kt \tag{2}$$

where α is the fraction of weight loss at the reaction time t, k is the rate constant, and $f(\alpha)$ and $g(\alpha)$ are functions describing the reaction mechanisms. Typical theoretical model functions $g(\alpha)$ for solid state reactions are shown in Table I [6]. Each $f(\alpha)$ can be calculated from $g(\alpha)$.

3.3. ISOTHERMAL STUDIES

Figure 2 shows a plot of the fraction of weight loss α, against time t of the reaction at constant temperature. For a given experimental curve, for example, the curve at 210 °C, a series of points (α, t) can be obtained. For a given model function in Table I, for example, D_1, $g(\alpha) = \alpha^2$, a series of points $[g(\alpha), t]$ can be calculated. The mechanism function suitable for experimental curves can be judged by the linearity of a plot of $g(\alpha)$ against time t. Taking the data at 210 °C and 220 °C as examples, Table II lists the linear regression results of $g(\alpha)$ versus t.

In the table, k is the rate constant and r is the correlation coefficient. The correct mechanism should have good linearity of $g(\alpha)$ versus t. Table II shows that the diffusion mechanisms have almost equally good linearity not only at 200 °C but at 220 °C. The statistical analyses obtained from the linear regression at 200 °C and 230 °C also support this result. Therefore all other mechanisms should be abandoned. It is difficult to distinguish precisely between mechanisms D_1, D_2, D_3 and D_4 on the basis of linearity alone.

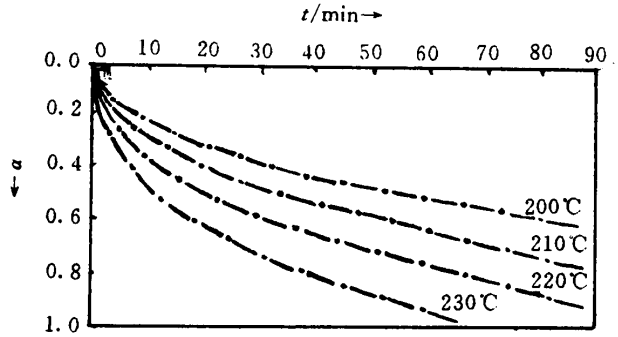

Figure 2. Isothermal weight loss curves of β-CD·C_9H_8O.

Table II. The linear regression fit to the dissociation of β-CD·C_9H_8O (210 °C, 220 °C).

210 °C			220 °C	
$g(\alpha)$	k/min^{-1}	r	k/min^{-1}	r
D_1	3.100×10^{-3}	0.9988	7.192×10^{-3}	0.9930
D_2	2.312×10^{-3}	0.9990	5.599×10^{-3}	0.9909
D_3	7.655×10^{-4}	0.9980	1.694×10^{-3}	0.9960
D_4	5.872×10^{-4}	0.9984	1.449×10^{-3}	0.9932
Au	1.345×10^{-2}	0.9570	3.420×10^{-3}	0.9468
R_1	3.254×10^{-3}	0.9737	7.994×10^{-3}	0.9513
R_2	2.335×10^{-3}	0.9868	5.751×10^{-3}	0.9698
R_3	1.761×10^{-3}	0.9900	4.341×10^{-3}	0.9743
A_1	6.780×10^{-3}	0.9949	7.685×10^{-3}	0.9891
A_2	4.047×10^{-3}	0.9799	2.432×10^{-3}	0.9659
A_3	2.874×10^{-3}	0.9722	7.141×10^{-3}	0.9499
A_4	2.222×10^{-3}	0.9670	6.213×10^{-3}	0.9436

3.4. NON-ISOTHERMAL STUDIES

Figure 3 shows the TG and DTG heating curve of β-CD·C_9H_8O. For a non-isothermal process:

$$\frac{\mathrm{d}\alpha}{\mathrm{d}T} = \frac{A}{\beta} e^{-E/RT} f(\alpha) \tag{3}$$

where A is the pre-exponential factor, E is the apparent activation energy, and β is the heating rate. It should be remembered that the peak height of DTG curves is not the actual value of $\mathrm{d}\alpha/\mathrm{d}T$. The actual reaction rate, $\mathrm{d}\alpha/\mathrm{d}T$, at a certain moment

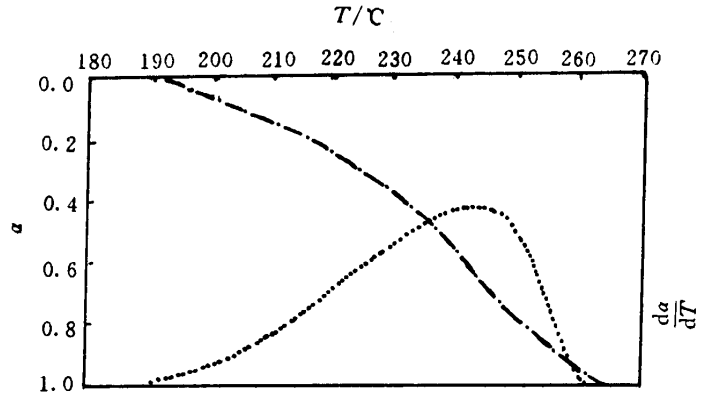

Figure 3. TG and DTG curves of β-CD·C_9H_8O heating rate, 5 °C min^{-1}.

may be determined graphically or more accurately by numerical differentiation. Rearranging Equations (3) and taking logarithms we get

$$\ln\left(\frac{\mathrm{d}\alpha}{\mathrm{d}T}\cdot\frac{1}{f(\alpha)}\right)=-\frac{E}{R}\cdot\frac{1}{T}+\ln\frac{A}{\beta}. \tag{4}$$

E and A can be determined from a linear regression fit of $\ln[(\mathrm{d}\alpha/\mathrm{d}T)\cdot(1/f(\alpha)]$ against $1/T$. The results are shown in Table III. In an isothermal process, from the Arrhenius equation $\ln k=\ln A-(E/R)\cdot(1/T)$, the related kinetic parameters can conveniently be obtained from a linear regression fit of $\ln k$ versus $1/T$, see Table III.

Comparing the correlation coefficient r in Table III, the diffusion mechanisms also have good linearity. Theoretically, for a given model function, the kinetic parameters obtained from the isothermal method should correspond with those from the non-isothermal method [7]. It is obvious that only D_1 and D_2 are possible mechanisms.

In order to select the most probable mechanism from D_1 and D_2, Criado's standard curves method at linearly increasing temperature was considered [8].

From Equation (3) Criado advanced a simple and high-speed analytical method, such that

$$\left(\frac{T}{T_{0.5}}\right)\frac{\mathrm{d}\alpha/\mathrm{d}t}{(\mathrm{d}\alpha/\mathrm{d}t)_{0.5}}=\frac{f(\alpha)g(\alpha)}{f(0.5)g(0.5)}, \tag{5}$$

where $T_{0.5}$ is the temperature at $\alpha=0.5$, and $(\mathrm{d}\alpha/\mathrm{d}t)_{0.5}$ is the rate of weight loss at $\alpha=0.5$, $f(0.5)$ and $g(0.5)$ are the values of corresponding functions at $\alpha=0.5$.

The right-hand side of Equation (5) only relates to the mechanism function. The plot of $[f(\alpha)g(\alpha)]/[f(0.5)g(0.5)]$ versus α will give a series of standard curves as shown in Figure 4. The left-hand side of Equation (5) can be obtained from

Table III. The kinetic parameters from non-isothermal and isothermal methods.

non-isothermal method				isothermal method	
$g(\alpha)$	E/kJ min^{-1}	A/min^{-1}	r	E/kJ min^{-1}	A/min^{-1}
D_1	147.47	2.41×10^{14}	0.9925	159.62	5.765×10^{14}
D_2	153.36	2.31×10^{14}	0.9981	160.15	8.01×10^{14}
D_3	202.24	3.49×10^{19}	0.9967	157.44	8.65×10^{13}
D_4	181.96	5.00×10^{16}	0.9980	158.71	3.64×10^{14}
Au	89.72	4.36×10^{7}	0.8950	–	–
R_1	61.98	2.78×10^{5}	0.9783	167.14	4.62×10^{15}
R_2	90.91	4.75×10^{8}	0.9924	170.74	6.76×10^{15}
R_3	81.31	3.98×10^{7}	0.9905	170.20	7.55×10^{15}
A_1	119.83	8.69×10^{11}	0.9860	159.28	1.13×10^{15}
A_2	64.50	7.44×10^{5}	0.9694	158.77	8.94×10^{13}
A_3	45.98	6.00×10^{3}	0.9501	165.96	2.53×10^{15}
A_4	38.36	4.14×10^{2}	0.9298	167.12	2.61×10^{15}

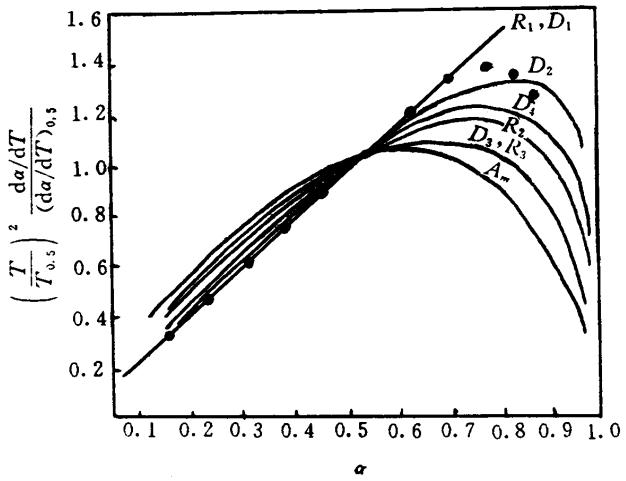

Figure 4. Criado standard curves • experiment points.

the DTG curve. The plot of $(T/T_{0.5})^2[(\mathrm{d}\alpha/\mathrm{d}t)/(\mathrm{d}\alpha/\mathrm{d}t)_{0.5}]$ against α will give an experimental curve. The values of $(T/T_{0.5})^2[(\mathrm{d}\alpha/\mathrm{d}t)/(\mathrm{d}\alpha/\mathrm{d}t)_{0.5}]$ related to various α were calculated from DTG curves, and a series of experimental points were obtained, as shown in Figure 4. The results denote that those points at $\alpha < 0.75$ fell almost entirely on curves R_1 and D_1. The deviations at $\alpha > 0.8$ probably were caused by the different size of the sample, because when $\alpha > 0.8$ the reactions of the smaller particles were completed and the reaction rate reduced. Considering the above analysis results, we conclude that the dissociation of β-CD·C_9H_8O is mainly dominated by mechanism D_1.

4. Crystal Structure Analysis

Thermal analysis is a useful means of elucidating the dynamic processes of the solid state reaction. Considering the effects of the errors in measurements and in mathematical treatment, the final mechanism obtained by pure mathematic analysis is doubtful. As a case in point, the kinetic parameters and mechanisms reported by different authors are often different [9, 10]. We believe that these effects should be eliminated by the combination of two or three methods. Naturally, the results concluded from thermal analysis should be examined by other techniques. All of the model functions for solid state reaction are based upon the crystal structure. The mechanism for dissociation of β-CD·C_9H_8O should also be suitably explained from the crystal structure of β-CD·C_9H_8O. The detailed structural analysis of β-CD·C_9H_8O is beyond the scope of this paper and therefore only some of the related structural information is considered.

Scanning electron microscopic observations on the samples and the products show that the size and the prism structure do not undergo any change during the dissociation process. This indicates that the crystals do not break into pieces in the heating process. In many β-CD complexes, two β-CD molecules are coupled to form a head-to-head dimer with the secondary hydroxyl sides facing each other. The dimers, stacking one by one, form tubular-type structures [11, 12]. Due to crystal anisotropy, the rate of reaction is different in different directions. In the dissociation of β-CD·C_9H_8O, the cinnamic aldehyde molecules escaping from β-CD cages move towards the crystal surface along the tubular directions. This process is similar to the successive reaction. The cinnamic aldehyde molecule escapes from one β-CD cage and passes into the adjacent β-CD cavity, and then gradually moves towards the surface.

It has been reported that the complexing process between cyclodextrins and guest molecules occurs approximately at the diffusion rate in solution [3]. It has also been confirmed that the stable energy of inclusion complexes of CD with weakly polar guest molecules consists mainly of van der Waals energy [13, 14]. The escape of guest molecules from a β-CD cavity is easy. So neither the nucleation nor the reaction at the phase boundary are the rate-limiting steps. In other words, the dissociation of β-CD·C_9H_8O is dominated by a diffusion mechanism, D_1. It is imaginable that β-CD molecules should not arrange in order at higher temperature, and the tubular-type structure may be diverged. This is the main reason that experimental points, when $\alpha > 0.8$, deviate from the D_1 mechanism in Criado standard curves.

5. Conclusions

β-CD can form a stable inclusion complex with cinnamic aldehyde, β-CD·C_9H_8O·$7H_2O$. The initial dissociation temperature of cinnamic aldehyde from β-CD is 200 °C. Before the decomposition of β-CD, cinnamic aldehyde molecules can

completely escape from β-CD cavity. The dissociation of β-CD·C_9H_8O is dominated by a D_1 mechanism. The apparent activation energy E is 160 kJ mol^{-1}. The pre-exponential factor is 5.8×10^{14} min^{-1}.

References

1. D. Dominque and W. Denis: *Acta Pharm. Technol*. **36**, 1 (1990).
2. S.K. Samant and J.S. Pai: *Indian Food Packer* **45**(3), 55 (1991).
3. J.F. Wojcik *et al.*: *J. Phys. Chem.* **79**, 2251 (1975).
4. W. Hirsch *et al.*: *Anal. Lett.* **22**, 2861 (1989).
5. K. Harata *et al.*: *Bull. Chem. Soc. Jpn.* **58**, 1234 (1985).
6. Y.Z. Li: *Thermal Analysis*, Qing Hua University Press, Bejing, 94–97 (1987).
7. T.P. Bagchi: *Thermochim. Acta* **51**, 175 (1981).
8. J.C. Criado: *Thermochim. Acta* **24**, 186 (1978).
9. C. Rozycki and M. Maciejewski: *Thermochim. Acta* **122**, 339 (1987).
10. S.G. Sinha and N.D. Deshapnde: *Thermochim. Acta* **156**, 1 (1989).
11. F. Nishioka, I. Nakanishi, T. Fujiwara, and K. Tomita: *J. Incl. Phenom.* **2**, 701 (1984).
12. I. Nakanishi, M. Arai, T. Fujiwara, and K. Tomita: *J. Incl. Phenom.* **2**, 689 (1984).
13. T.X. Liu *et al.*: *J. Chem. Soc. Faraday Trans.* **85**(2), 1439 (1989).
14. Y. Mastui *et al.*: *Bull. Chem. Soc. Jpn.* **55**, 1246 (1982).